Reprinted with permission from
ANNALS OF NONINVASIVE ELECTROCARDIOLOGY, Volume 5, No. 2, April 2000

Detection of Exercise-Induced Myocardial Ischemia by Multichannel Magnetocardiography in Single Vessel Coronary Artery Disease

Helena Hänninen, M.D.,*† Panu Takala, M.Sc.,†‡
Markku Mäkijärvi, M.D.,*† Juha Montonen, Ph.D.,†‡
Petri Korhonen, M.D.,*† Lasse Oikarinen, M.D.,*†
Jukka Nenonen, Ph.D.,†‡ Toivo Katila, Ph.D.,†‡
and Lauri Toivonen, M.D.*†

*From the *Division of Cardiology and †BioMag Laboratory, Helsinki University Central Hospital, and ‡Laboratory of Biomedical Engineering, Helsinki University of Technology, Helsinki, Finland*

Background: Detection of myocardial ischemia was studied with multichannel exercise magnetocardiography (MCG). A surface gradient method was applied to analyze cardiac magnetic fields.

Methods: We studied 27 patients with single vessel coronary artery disease (CAD) and 17 healthy volunteers. The MCG was recorded over anterior chest during supine bicycle ergometry. The two-dimensional direction of the maximum spatial magnetic field gradient was determined during the ST segment and at the T-wave apex at different phases of stress test.

Results: The CAD patient group was separated from controls by the orientation of the magnetic field gradient during the ST segment at cessation of exercise (CAD 167 ± 68° vs controls 106 ± 49°; $P < 0.005$) and at 4 minutes postexercise, but not at rest. The CAD patient group was separated from controls also by the orientation of the magnetic field gradient at the T-wave apex at 4 minutes postexercise (CAD 87 ± 60° vs controls 58 ± 18°; $P < 0.05$), but not at rest. The change in the orientation of the field gradient at the T-wave apex 4 minutes postexercise, compared to baseline, was greater in CAD patients (31 ± 43°) than in controls (9 ± 8°; $P < 0.05$). This change was larger in the patient group with stenosis in the right than in the left coronary artery ($P < 0.05$).

Conclusions: Transient acute myocardial ischemia causes well-recognizable changes in the magnetocardiogram at the ST segment and the T wave. The orientation of the maximum spatial gradient of the magnetic field can be used as a parameter to determine these changes.

A.N.E. 2000;5(2):147–157

magnetocardiography; noninvasive cardiac mapping; coronary artery disease; myocardial ischemia; exercise testing; repolarization

Accurate detection, localization, and quantification of myocardial ischemia is important for applying therapeutic interventions in coronary artery disease (CAD). In clinical practice, the diagnosis of coronary artery disease can be affirmed by several noninvasive techniques: exercise electrocardiography, radionuclide methods, magnetic resonance imaging, stress echocardiography, and positron emission tomography.[1-7] The increasing possibilities of treatment for CAD patients require fast and preferably noninvasive techniques to evaluate the extent and location of the ischemic myocardial target area to be treated.

Magnetocardiography (MCG) is a novel noninva-

This work was supported by Finnish Cardiac Research Foundation and Aarne Koskelo Foundation.
Address for reprints: Helena Hänninen, M.D., Helsinki University Central Hospital, Division of Cardiology, Haartmaninkatu 4, FIN 00290 Helsinki, Finland. Fax: +358 9 4717 4574; E-mail: hahannin@sci.fi

Table 1. Characteristics of Study Groups

Subgroup	CAD Group				Control Group Total
	Total	LAD	LCX	RCA	
Number	27	12	7	8	17
Age (years)	58 ± 10	57 ± 10	61 ± 7	58 ± 12	55 ± 7
Male/Female	15/12	6/6	4/3	5/3	12/5
LVEF (%)	65 ± 8	64 ± 6	70 ± 8	62 ± 8	66 ± 7
Stenosis (%)	86 ± 13	81 ± 15	91 ± 12	92 ± 5	—

Number of study subjects or mean ± SD. CAD = coronary artery disease patients; LVEF = left ventricular ejection fraction; LAD = patients with left anterior descending coronary artery stenosis; LCX = patients with left circumflex coronary artery stenosis; RCA = patients with right coronary artery stenosis.

sive multichannel mapping technique to record cardiac electromagnetic signals generated by the same ionic currents underlying the ECG.[8] The MCG has similar morphological features to the ECG, such as QRS complex, T, P, and U waves, but there are some fundamental differences. The MCG is more sensitive to tangential currents in the heart than the ECG, and it is also sensitive to vortex currents, which cannot be detected by the ECG.[8] In normal heart, the main direction of the activation wavefront is radial, from endocardium to epicardium. For these reasons, MCG may show ischemia-induced deviations from the normal direction of depolarization and repolarization with better accuracy than the ECG. The magnetic signal is less dependent than electric on variation of conductance in body structures like lungs, muscles, and skin.[9-11] In addition, MCG is a totally noncontact method, and the problems of the skin-electrode contact of the ECG are avoided.[9-11] To improve signal-to-noise ratio, the very sensitive MCG recordings are performed in a magnetically shielded room.[12]

Ischemic ST-segment depressions have been found in the MCG of a coronary artery disease patient after physical stress.[13] In the direct current MCG of a CAD patient during exercise, the ST segment became depressed and the baseline TQ segment elevated, and in experimental myocardial infarction these changes were the opposite, both only detectable in the direct current MCG but not in the ECG.[14-16] MCG has also been shown to carry independent complementary information compared to body surface potential mapping in patients with ischemic heart disease.[17]

The purpose of the present study was to assess the ability of multichannel MCG to detect and localize exercise-induced myocardial ischemia in patients with well-defined coronary artery disease. For the assessment of the ischemia-induced changes in the multichannel MCG we introduce a computer-based technique, the surface gradient method.

METHODS

Patients and Controls

The study population (Table 1) consisted of 44 subjects: 27 patients with single vessel coronary artery disease and 17 healthy volunteers. All patients had significant (>50% luminal diameter) stenosis in one of the main coronary branches (left anterior descending coronary artery, LAD; left circumflex coronary artery, LCX; or right coronary artery, RCA) in the coronary arteriogram (Table 1). At screening, all patients were required to have anginal pain and ECG-documented evidence of ischemia with ≥ 0.1 mV ST-segment depression in symptom-limited upright bicycle ergometry. It was also required that none of the patients had suffered a transmural myocardial infarction, did not show abnormal Q waves, had normal left ventricular function in cine angiography, and had no left ventricular hypertrophy in echocardiography. All patients were clinically stable and under appropriate medication during the study: 25 patients were on β-blockers, 6 patients on calcium antagonists, and 21 patients on long-acting nitrates. There was no significant difference in weight, height, or body surface area between the CAD patients and controls. The healthy controls had no history of hypertension, smoking, or heart disease in the family, and had normal findings on transthoracic echocardiography as well as bicycle ergometry. Before in-

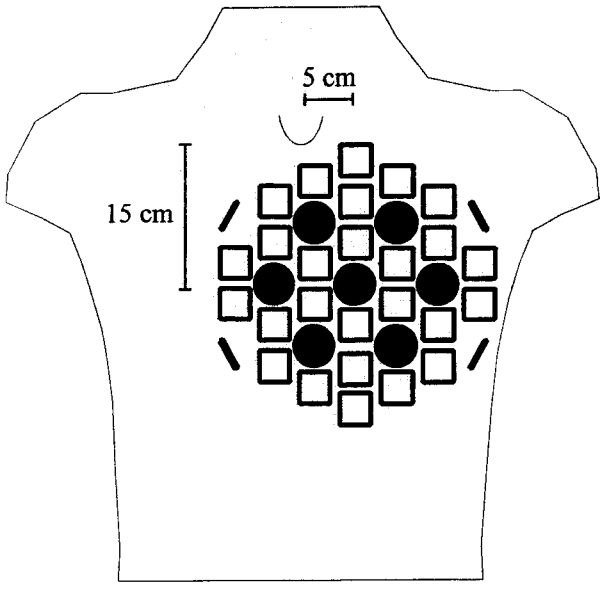

Figure 1. The sensor arrangement in the 67-channel cardiomagnetometer. The XY plane is parallel to the sensor surface, while the Z coordinate points into the chest. The circles refer to the seven coaxial gradiometers, while each rectangle has two orthogonal planar gradiometers.

clusion, all patients and controls gave their informed consent for the study.

Magnetocardiography

A 67-channel magnetometer was used (Neuromag Ltd., Helsinki, Finland) for the MCG recordings, which were performed in a magnetically shielded room (Euroshield Ltd., Eura, Finland) of the BioMag Laboratory in a hospital environment.[12] The sensors, 7 co-axial and 60 planar dc-SQUID (Superconducting Quantum Interference Device) gradiometers, record the spatial change in the magnetic field component perpendicular to the measurement plane (B_Z) (Fig. 1). The gradiometers are arranged on a slightly curved surface with a diameter of 30 cm and immersed in liquid helium inside a dewar. The dewar is supported by a gantry, allowing easy adjustment of the sensor array both in a horizontal and vertical direction and also tilting. During the measurement, the patient is lying on a nonmagnetic bed. The center of the cardiomagnetometer sensor array is placed 15 cm down from the jugular notch and 5 cm to the left of the midsternal line, as close to the chest as possible without touching the patient (Fig. 1). All recordings were band-pass filtered to 0.03-300 Hz and digitized with a sampling frequency of 1000 Hz.

First, a baseline recording was done in a resting state for 5 minutes. Supine bicycle exercise test was then performed using a nonmagnetic ergometer designed and constructed for stress MCG recordings. It was calibrated against a bicycle stress ergometer (Siemens Ergomed 840L, Germany) used in the cardiac catheterization laboratory for supine exercise testing. During exercise, the workload was increased stepwise and blood pressure monitored every 2 minutes. The cessation criteria were severe fatigue or dyspnea, severe chest pain, progressive decrease or abnormal elevation of systolic blood pressure, or repetitive ventricular arrhythmias. The MCG and the 12-lead ECG were continuously recorded during the exercise and ten minutes after the cessation of exercise. The rate pressure products in the stress testing were calculated as the product of the maximum systolic blood pressure (mmHg) and maximum heart rate (beats/min) divided by 100.

The study was performed according to the Declaration of Helsinki, and was approved by the local ethics committee.

MCG Analysis

The MCG signals were baseline corrected and averaged to increase the signal-to-noise ratio. In the averaging process, a line fitted to the PQ and TP intervals was subtracted from the raw data of each cardiac cycle to define the baseline level. In case of high heart rate, resulting in a shortened TP segment, a line connecting two consecutive PQ intervals was used as a baseline. Four different phases of the exercise test were used in the analysis: (1) rest, (2) cessation of exercise, (3) 2 minutes and (4) 4 minutes postexercise. Two time intervals chosen for the analysis were determined using the signals of coaxial gradiometers (Fig. 2): (1) an integral of the second quarter from the J-point to the T-wave apex representing ST-segment, and (2) the T-wave apex. Magnetic isofield maps were formed at these time intervals using the signal-averaged MCG as described in the Appendix.

For the determination of magnetic field orientation the so-called surface gradient method was developed, based on the arrow maps introduced by Cohen et al.[18] First the spatial difference of the magnetic field perpendicular to the measurement plane (B_z), named surface gradient, was calculated,

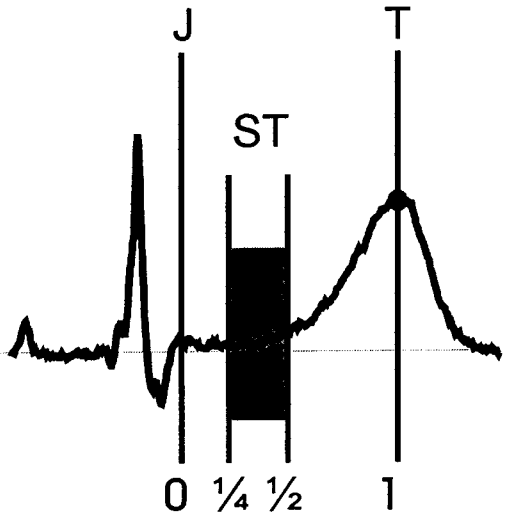

Figure 2. The analyzed instants of the cardiac cycle were the ST segment as an integral of the second quarter from the J point to the T-wave apex, and the T-wave apex.

as described in the Appendix. The two-dimensional orientation of the largest, peak surface gradient was used as a parameter for further analysis. This orientation was determined during the ST segment and at the T-wave apex at different phases of stress testing. In addition, manual evaluation of the isofield maps was performed by drawing a line from the magnetic field minimum to the field maximum to determine the orientation of the field polarity. This was also done during ST segment and at the T wave apex at the same phases of stress testing (Figs. 3 and 4).

In dipolar magnetic field maps, the peak gradient is located close to the zero line between the extrema of the spatial magnetic field (Appendix, Fig. A1). The changes in the magnetic field induced by myocardial ischemia were quantified by the change in the orientation of the peak gradient and field polarity. Occasionally, monopolar or strongly asymmetric bipolar magnetic maps were found where both extrema of the field could not be seen. Even in such cases, the line connecting the largest and smallest field value was usually parallel to the peak gradient calculated. In cases of almost monopolar field maps, the rotation of the extrema cannot be determined. The direction of the peak

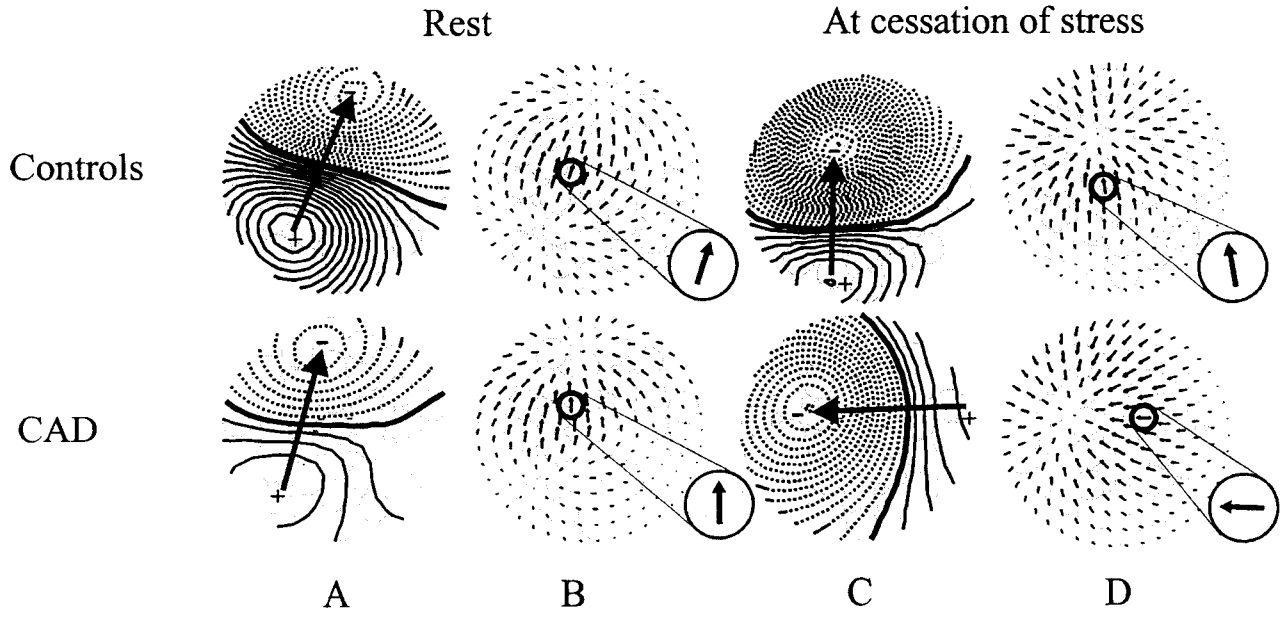

Figure 3. The group mean ST-segment magnetic field distribution and interpolated spatial field gradient of 17 healthy controls and 27 coronary artery disease patients (CAD) at rest and at cessation of exercise. Spatial distribution of the magnetic field component B_z at rest (A) and at cessation of exercise (C). The line connecting the magnetic field maximum and minimum is marked by an arrow. The change in the magnetic field orientation can be seen as a rotation of the arrow. Interpolated gradient arrows at rest (B) and at cessation of exercise (D). The peak gradient is marked by a circled arrow, which is enlargened. The map direction in A and C parallels the direction of the maximal field gradient in B and D, respectively. Continuous line = positive field distribution; dotted line = negative field distribution, the step between two consecutive lines is 0.1 pT.

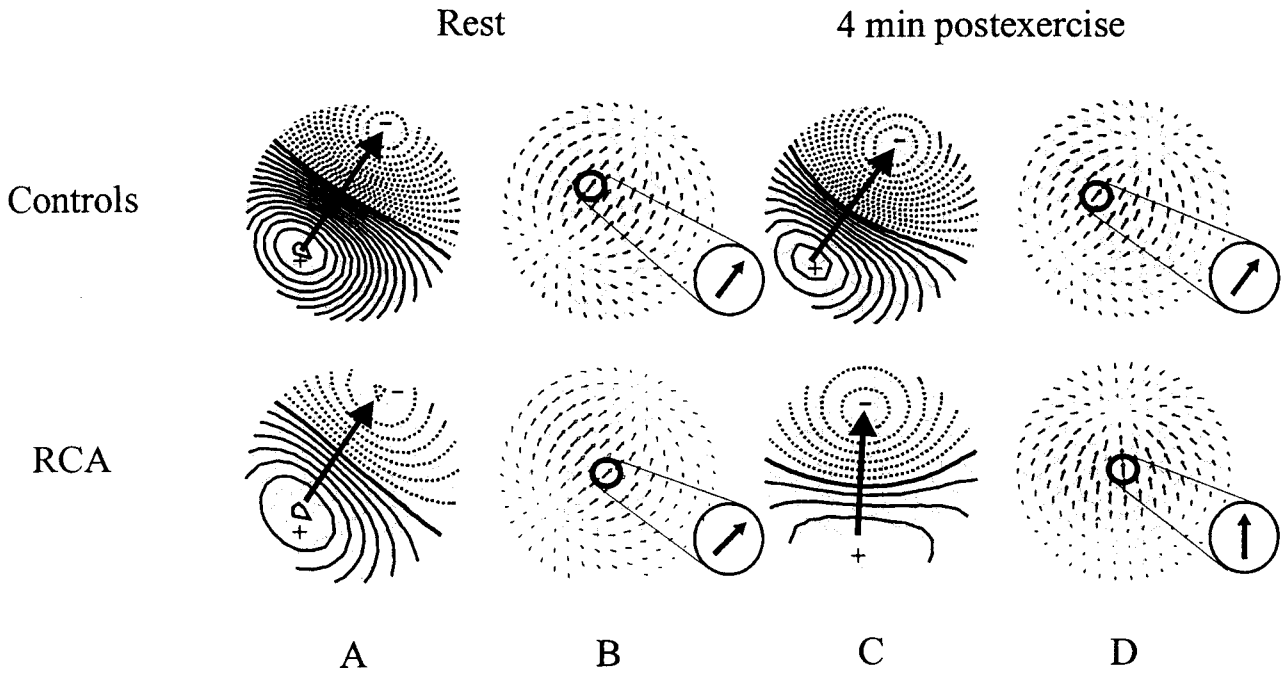

Figure 4. The group mean T-wave apex magnetic field distribution and interpolated spatial field gradient of 17 healthy controls and 8 patients with stenosis in the right coronary artery (RCA) at rest and 4 minutes postexercise. Spatial distribution of the magnetic field component B_z at rest (A) and 4 minutes postexercise (C). Interpolated gradient arrows at rest (B) and 4 minutes postexercise (D). Technical description is the same as Figure 2 for the ST segment. The step between two consecutive lines is 0.5 pT

gradient, however, also indicates the orientation of the magnetic field in such cases.

Definitions

Surface field gradient: two-dimensional direction and magnitude of spatial difference in magnetic field perpendicular to the measurement plane (B_z).

Peak field gradient, peak gradient: the largest surface gradient detected over the mapped area.

Orientation of the peak gradient: angle between the peak gradient and a horizontal axis pointing on the patients left on the measurement plane.

Rotation of the peak gradient: change in the orientation of the peak gradient between different phases of stress test and at the resting state.

Orientation of the field polarity: angle between the line connecting the magnetic field minimum and maximum and a horizontal axis pointing on patients left on the measurement plane.

Rotation of the field polarity: the change in the orientation of the field polarity between different phases of stress test and at the resting state.

Statistical Analysis

The statistical analysis of parameters was carried out using the Mann-Whitney U test. A two-tailed P value < 0.05 was considered statistically significant.

RESULTS

In CAD patients and controls the magnetic field at rest was weak during ST segment, with a signal intensity often below 0.1 pT. This matched with the isoelectric ST segment in the ECG. During stress studies, the magnetic field of the ST segment was enhanced in CAD patients and controls, and the maximum ST-segment depression amplitude was not different between the groups. The orientation of the ST-segment magnetic field did not separate the CAD patient group from controls at rest. Due to the weak signals at rest, easily disturbed by measurement noise, only the orientation

Table 2. Orientation of ST-Segment Peak Gradient in Degrees (Mean ± SD) and Statistical Significance of CAD Patient Groups Compared to Control Group

Group	Rest	P Value	Cessation of Exercise	P Value	4 Min Postexercise	P Value
Controls	88 ± 60	—	106 ± 49	—	112 ± 50	—
CAD	119 ± 94	NS	167 ± 68	<0.005	160 ± 43	<0.005
LAD	102 ± 73	NS	191 ± 56	<0.01	150 ± 41	<0.05
LCX	92 ± 119	NS	130 ± 79	NS	184 ± 38	<0.01
RCA	168 ± 91	<0.01	165 ± 66	<0.05	157 ± 48	NS

CAD = coronary artery disease patients; LAD = patients with left anterior descending coronary artery stenosis; LCX = patients with left circumflex coronary artery stenosis; RCA = patients with right coronary artery stenosis.

of the magnetic field at cessation of stress and at different phases of recovery was used for the further analysis of the ST segment. The magnetic field during T wave is stronger also at rest. Therefore, the T-wave apex could be analyzed reliably at rest and at different phases of recovery.

Coronary Artery Disease Patients and Controls

The CAD patient group was separated from controls by the orientation of the peak gradient during the ST segment at cessation of exercise (CAD 167 ± 68° vs controls 106 ± 49°; $P < 0.005$) and also 4 minutes postexercise (Fig. 3 and Table 2). Similar results were also found in the manual measurement of the orientation of the field polarity during the ST segment, where the CAD patient group was separated from controls at cessation of exercise (CAD 167 ± 54° vs controls 104 ± 54°; $P < 0.005$) and also 4 minutes postexercise ($P < 0.01$).

The orientation of the peak gradient at the T-wave apex 4 minutes postexercise was different in the CAD patient group compared to controls (CAD 87 ± 60° vs controls 58 ± 18°; $P < 0.05$) (Fig. 4 and Table 3). Also the rotation of the peak gradient at the T-wave apex was larger in the CAD patient group than in controls at 4 minutes postexercise (CAD 31 ± 43° vs controls 9 ± 8°; $P < 0.05$) (Fig. 4 and Table 4). At 4 minutes postexercise both the manually measured orientation of the field polarity and it's rotation at the T-wave apex separated CAD patient group from controls (for the T-wave orientation CAD 81 ± 52° vs controls 55 ± 19°; $P < 0.05$). The findings at 2 minutes postexercise resembled those at 4 minutes postexercise although in general less pronounced.

Patient Subgroups versus Controls

The orientation of the peak gradient during the ST segment separated the LAD patient subgroup from the control group after stress (at cessation of stress: LAD 191 ± 56° vs controls 106 ± 49°; $P < 0.01$) (Figs. 3 and 5 and Table 2). Also the orientation of the field polarity during the ST segment in the manual measurement was different in the LAD patient subgroup than in controls at cessation of exercise (LAD 169 ± 55° vs controls 104 ± 54°; $P < 0.01$).

Table 3. Orientation of T-Wave Peak Gradient in Degrees (Mean ± SD) and Its Statistical Significance Comparing Patient Groups to Controls

Group	Rest	P Value	Cessation of Exercise	P Value	4 Min Postexercise	P Value
Controls	56 ± 12	—	61 ± 19	—	58 ± 18	—
CAD	65 ± 61	NS	66 ± 44	NS	87 ± 60	<0.05
LAD	54 ± 15	NS	57 ± 22	NS	82 ± 61	NS
LCX	48 ± 16	NS	50 ± 21	NS	86 ± 82	NS
RCA	97 ± 109	NS	94 ± 68	NS	97 ± 42	<0.05

Mann-Whitney U-test. CAD = coronary artery disease patients; LAD = patients with left anterior descending coronary artery stenosis; LCX = patients with left circumflex coronary artery stenosis; RCA = patients with right coronary artery stenosis.

Table 4. Change in Orientation (Rotation) of the T-Wave Peak Gradient Compared to Resting State in Degrees (Mean ± SD) and Its Statistical Significance Comparing Patient Groups to Controls

Group	Cessation of Exercise	P Value	4 Min Postexercise	P Value
Controls	9 ± 10	—	9 ± 8	—
CAD	17 ± 20	NS	31 ± 43	<0.05
LAD	12 ± 10	NS	24 ± 42	NS
LCX	14 ± 12	NS	29 ± 49	NS
RCA	29 ± 31	<0.05	45 ± 39	<0.005

CAD = coronary artery disease patients; LAD = patients with left anterior descending coronary artery stenosis; LCX = patients with left circumflex coronary artery stenosis; RCA = patients with right coronary artery stenosis.

The orientation of the ST-segment peak gradient 4 minutes postexercise (LCX 184 ± 38° vs controls 112 ± 50°, $P < 0.01$) separated LCX patient subgroup from controls (Fig. 5 and Table 2). In the LCX patient subgroup the isofield map during ST segment became monopolar after stress (Fig. 5).

The orientation of the peak gradient of the ST segment separated the RCA patient subgroup from controls at cessation of stress (RCA 165 ± 66° vs controls 106 ± 49°, $P < 0.05$) (Fig. 5 and Table 2). The angle and the rotation of the peak gradient at the T-wave apex was larger in the RCA patients than in the controls 4 minutes postexercise (Tables 3 and 4). At 4 minutes postexercise the RCA patient subgroup was separated from controls in manual measurement of the orientation and the rotation of

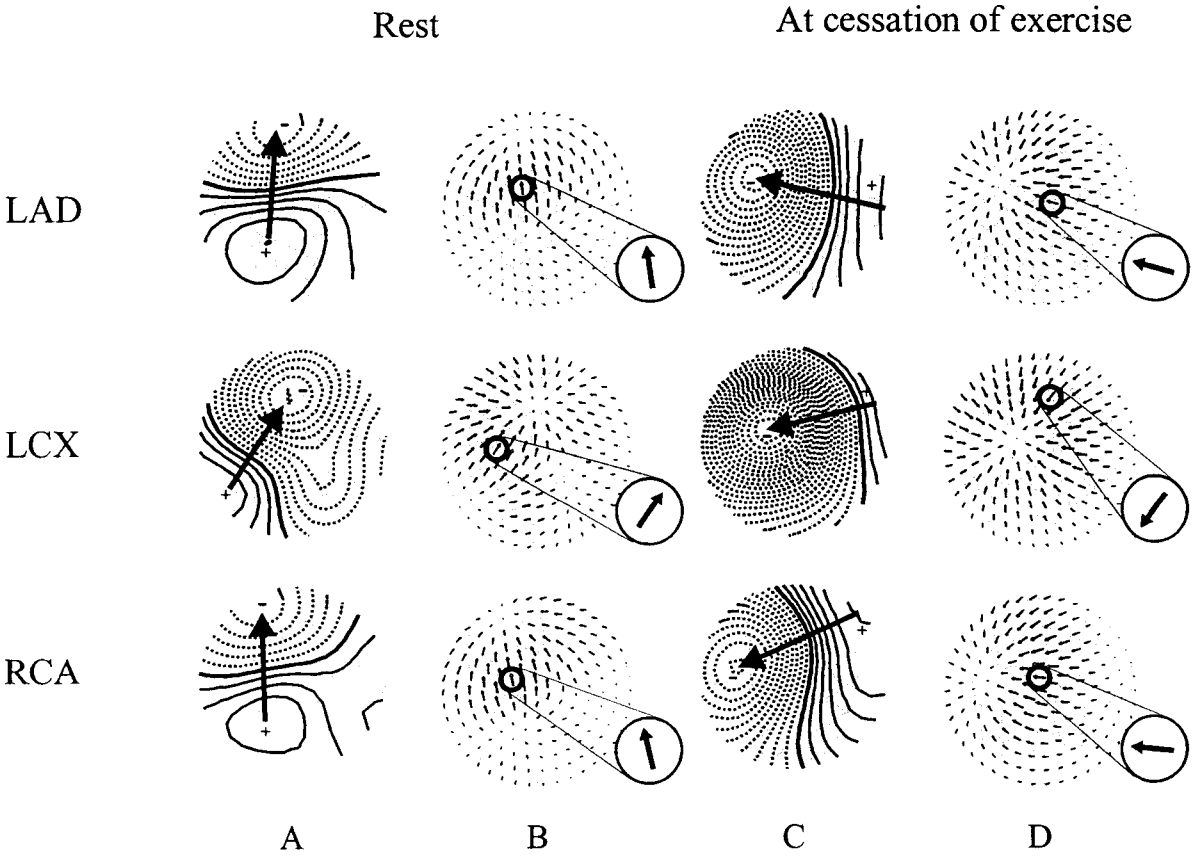

Figure 5. The group mean ST-segment magnetic field distribution and interpolated spatial field gradient of 12 patients with stenosis in the left anterior descending coronary artery (LAD), 7 patients with stenosis in left circumflex coronary artery (LCX), and 8 patients with stenosis in right coronary artery (RCA) at rest and at cessation of stress. Spatial distribution of the magnetic field component B_z at rest (A) and at cessation of stress (C). Interpolated gradient arrows at rest (B) and at cessation of exercise (D). Technical description is same as for Figure 2. The rotation of the magnetic field of the ST segment from rest to the immediate postexercise period is seen in all patient groups compared to controls (see Fig. 3 for the controls). In the LCX patient group, the isofield map became monopolar after stress. The step between two consecutive lines is 0.1 pT.

the field polarity at the T-wave apex (for the T-wave orientation RCA 95 ± 36° vs controls 55 ± 19°; $P < 0.01$).

The LAD versus the RCA versus the LCX Patient Subgroup

At the T-wave apex 4 minutes postexercise the RCA patient group was separated from the LAD patient group by rotation of the peak gradient (RCA 45 ± 39° and LAD 24 ± 42°) (Table 4) and rotation of the field polarity (RCA 44 ± 33° and LAD 26 ± 48°) ($P < 0.05$ both). The rotation of the T-wave peak gradient was also larger in the RCA than in the LCX patient subgroup 4 minutes postexercise (RCA 45 ± 39° vs LCX 29 ± 49°, $P < 0.05$) (Table 4).

Comparison to Stress Electrocardiography

During supine stress testing 4 of 12 patients in the LAD group, 4 of 8 patients in the RCA group, and 4 of 7 patients in the LCX group (total: 12 of 27 patients) (44%) fulfilled the standard ischemia criterion of ≥ 0.1 mV ST-segment depression in the simultaneously recorded 12-lead ECG, although all patients had severe angina taking minutes to resolve. The maximum rate pressure products achieved at supine MCG stress testing were lower (CAD 184 ± 52 and controls 234 ± 57) than those achieved in the upright bicycle ergometry (CAD 245 ± 52 and controls 302 ± 42).

A subgroup analysis of the 12 patients fulfilling the ischemia criterion of 0.1 mV ST-segment depression in the simultaneously recorded 12-lead ECG was performed. The orientation of the ST-segment peak gradient at cessation of stress and the orientation and rotation of the T-wave apex peak gradient 4 minutes postexercise separated the subgroup of CAD patients from controls (ST-segment at cessation of stress: CAD 157 ± 55° vs controls 106 ± 49°; $P < 0.01$). The mean values for the magnetic field both in the ST segment and at the T-wave apex resembled those in the whole material.

DISCUSSION

The present study shows that the presence and location of acute transient myocardial ischemia can be detected in exercise magnetocardiography. Ischemia-induced changes were quantified as abnormalities in the orientation of the peak gradient of the precordial ST-segment and T-wave magnetic field. The orientation of the ST-segment magnetic field separated the CAD patient group from controls at cessation of exercise. The orientation of the T-wave apex magnetic field and its rotational change after stress was abnormal in the CAD patient group compared to controls. Demonstrating the capacity to localize ischemia, the rotation of the T-wave magnetic field postexercise was significantly larger in the RCA subgroup than in the LAD and LCX subgroups. In addition, the isofield map of ST segment in LCX patients became monopolar after stress.

In this first look of stress MCG data in patients with well-defined coronary stenoses we aimed to characterize some typical features for ischemia in MCG. Saarinen et al.[13] reported the first nondirect current MCG recording in a CAD patient, where both 12-lead ECG and single channel MCG from 3 different locations were recorded after physical stress. The ischemic postexercise ST changes were seen in ECG and MCG, but the ST-shift amplitude/R amplitude ratio was greater in MCG than in ECG.

In the study of van Leeuwen et al.[19] on healthy subjects, CAD patients with normal ECG, and postinfarction patients with abnormal ECG, the cardiac magnetic field during the QT interval was characterized by the field strength, field width, and field orientation defined as the location of the center of gravity. The MCG field orientation could separate the CAD patients and the postinfarction patients from healthy controls at rest, and these MCG changes were more prominent in patients with multivessel disease. MCG changes were also apparent in CAD patients with normal ECGs, implying that MCG at rest contains relevant additional information to ECG, possibly reflecting silent ischemia.

In our study, the orientation of the magnetic field peak gradient at rest could not identify the CAD patient group. Exercise-induced ischemia caused abnormalities in the orientation of the magnetic field immediately after stress during the ST segment and enhancing some minutes after the cessation of stress at the T-wave apex. The MCG was capable of detecting ischemia despite the poor performance of the 12-lead ECG, which fulfilled the standard ischemia criterion in only 44% of the patients in the same test situation. In addition, the changes observed in patient subgroups infer that

the ischemia criteria might not be the same for different myocardial regions supplied by the main coronary branches. In the supine position, the diastolic filling pressure of the ventricles is higher, stretching the ventricles during diastole, and therefore changing the dynamics of the coronary blood flow after the ischemic threshold.[20] The position of the heart also differs from that in the upright test with respect to the ECG recording locations, which might reduce the sensitivity of the ECG to detect ischemia-induced ST-segment and T-wave alterations. The supine test position also might have been disadvantageous for MCG.

Seese et al.[21] recorded MCG at rest in 5 patients with acute myocardial infarction and after physical stress testing in 11 patients with coronary artery disease. The minimum norm method was used for the construction of the current density during the ST segment. Injury currents during transient exercise-induced ischemia were in most cases directed from the ischemic area to the nonischemic area, whereas the injury currents in acute infarction flew in the opposite direction.

Lant et al.[17] reported the MCG and the body surface potential mapping to be complementary. The most profound abnormalities in the MCG maps in anterior myocardial infarction were found in the QRS complex, while abnormalities in inferior infarction were found during the entire repolarization period. On the contrary, the potential mapping showed significant differences between anterior and inferior infarctions during the QRS complex only. The repolarization abnormalities detected in MCG maps could have been caused by prolonged ischemic injury increasing tangential current flow through the spared subendocardial tissue.

Our study of CAD patients with no transmural myocardial infarction examined the MCG in transient, acute myocardial ischemia more specifically than the above mentioned,[17,19] where the depolarization and repolarization abnormalities caused by acute myocardial ischemia and previous myocardial infarction were mixed. Most profound abnormalities in the magnetic field at the T-wave apex also were found in our study in patients with inferior wall ischemia. The capability of MCG to detect ischemia in general and especially posterior ischemia and posterior myocardial infarction could be partly explained by the hypothesized tangential orientation of the ischemic injury currents.

In the present study, the amplitude of the ST-segment depression in MCG did not separate the CAD patients from controls. Therefore, magnetocardiographic evaluation of myocardial ischemia cannot be based solely on ST-segment amplitude changes similar to those used in the standard 12-lead ECG.[24] The magnetic field peak gradient orientation parameter introduced produces results resembling results in evaluation of the magnetic field orientation as the visual inspection of the field polarity. The automatic surface gradient method seems a useful technique for the evaluation of ischemia-induced changes in the magnetic field. Dynamic analysis of the magnetic field during the ST segment and the T wave at the creation of ischemia and its recovery is likely to further improve the detection and localization of myocardial ischemia.

LIMITATIONS OF THE STUDY

The patient material measured and analyzed in this study was relatively small, and therefore only preliminary conclusions can be drawn. Localization and quantification of ischemia by isotope ventriculography would have further improved the evaluation of the ischemic myocardial regions. However, the study patients selected had a well-defined ischemic region supplied by stenotic main coronary branch and had no abnormalities in the coronary anatomy that would affect the extent and location of the ischemic region. In addition, if only the patients with ischemia indication in the simultaneously recorded 12-lead ECG were taken into analysis, the results were concordant with the entire study group. This study did not assess ischemia detection in the presence of old myocardial infarction; however, myocardial scar did not confound the specificity to actual ischemia.

CONCLUSIONS

Exercise-induced myocardial ischemia causes significant changes in the magnetocardiogram of the coronary artery disease patient. Moreover, changes related to special phases of the cardiac repolarization enable approximate localization of the ischemic myocardial region. Changes in the ST-segment orientation are most profound immediately after cessation of stress, whereas those in the T wave emerge later. The MCG method used in the study seems to be especially sensitive to inferior wall ischemia detected by T-wave changes in the postexercise period. Dynamic analysis of car-

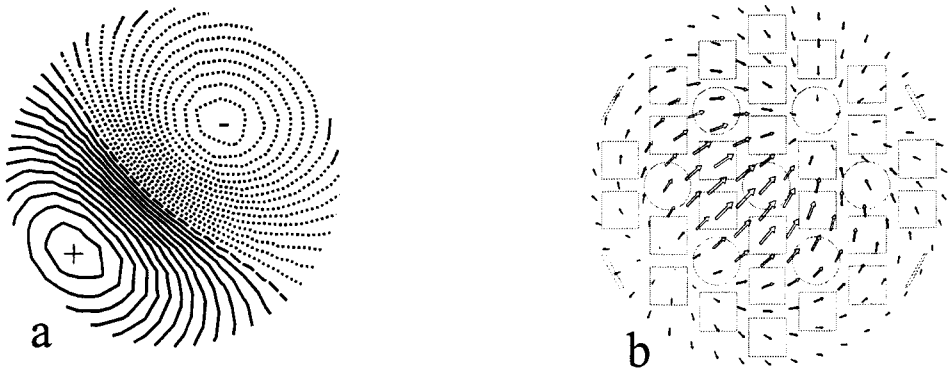

Figure A1. (a) Spatial distribution of the magnetic field component B_z, at T-wave apex, interpolated from the measurements using minimum-norm estimation. Thick lines indicate magnetic field flux into the chest (+), while thin contour lines denote flux out of the chest (-). The step between adjacent isocontour lines is 1 pT. (b) Interpolated gradient arrows corresponding to the isocontour map.

diac magnetic fields during provoked ischemia could make MCG a potential method to study the presence and locality of ischemia caused by coronary artery stenoses.

Acknowledgments: *The authors thank Ms. Rea Katajisto and Ms. Leila Sikanen for their technical assistance in the stress testing.*

APPENDIX: SPATIAL INTERPOLATION WITH MINIMUM-NORM ESTIMATION

In this work, the isocontour maps and surface gradients were interpolated from the measured data using minimum-norm estimation (MNE).[22] MNE is a current density field, $\mathbf{J}^*$, defined as a linear combination of the lead fields of the MCG sensors,

$$L_k: J^*(r) = \sum \omega_k L_k(r). \quad (1)$$

It is the current distribution that has the smallest norm and is compatible with the measured data. We define the next matrix Γ consisting of inner products between the lead fields of all sensor pairs L_i and L_j. Then, the weighting coefficients ω_k are found from the measured signals

$$b^m \text{ by } \omega = \Gamma^{-1} b^m \quad (2)$$

Because the lead fields in a large array are almost linearly dependent, regularization techniques are needed to produce stable estimates.[22]

Interpolation with MNE[23] is based on evaluating the lead fields of virtual sensors

$$L^s_{k,} \quad (3)$$

and composing matrix Γ' from the dot products between measurement and virtual lead fields. The interpolated signals are then obtained as $b^e = \Gamma'\Gamma^{-1} b^m$.

For isocontour and gradient interpolation, the sensor array surface (Fig. A1) was triangulated. The field component B_z perpendicular to the surface was interpolated at each time instant by assuming a virtual point coil detecting B_z at each node on the triangulated surface. Surface gradients $\partial B_z/\partial x$ and $\partial B_z/\partial y$ were interpolated by placing two virtual difference sensors at each node point.

REFERENCES

1. Tilkemeier PL, Katz AS, Parisi AF. The role of noninvasive testing in evaluating patients for coronary artery disease. Curr Opin Cardiol 1996;11:409-417.
2. Morise AP, Diamond GA, Detrano R, et al. Incremental value of exercise electrocardiography and thallium-201 testing in men and women for the presence and extent of coronary artery disease. Am Heart J 1995;130:267-276.
3. Ismail G, Lo E, Sada M, et al. Long-term prognosis of patients with a normal exercise echocardiogram and clinical suspicion of myocardial ischemia. Am J Cardiol 1995;75:934-935.
4. Sawada SG, Segar DS, Ryan T, et al. Echocardiographic detection of coronary artery disease during dobutamine infusion. Circulation 1991;83:1605-1614.
5. Marie P, Danchin N, Durand JF, et al. Long-term prediction of major ischemic events by exercise thallium-201 single photon emission computed tomography. J Am Coll Cardiol 1995;26:879-886.
6. Ho FM, Huang CS, Liau FK, et al. Dobutamine stress echo compared with dipyridamole thallium-201 single-photon emission computed tomography in detecting coronary artery disease. Eur Heart J 1995;16:570-575.
7. Brown K. Prognostic value of cardiac imaging in patients with known or suspected coronary artery disease: Comparison of myocardial perfusion imaging, stress echocardiography, and positron emission tomography. Am J Cardiol 1995; 75:35D-41D.

8. Siltanen P. Magnetocardiography. Chapter in MacFarlane P, (ed): Comprehensive Electrocardiology Volume II. New York, Pergamon Press, 1989, pp. 1405-1438.
9. Cohen D. Steady fields of the heart. Chapter in S J Williamson, G-L Romani, L Kaufman, et al. (eds.): Biomagnetism. An Interdisciplinary Approach. New York, Plenum, 1983, pp. 265-274.
10. Plonsey R. Comparative capabilities of electrocardiography and magnetocardiography. Am J Cardiol 1972;29:735-736.
11. Nenonen J. Solving the inverse problem in magnetocardiography. IEEE Eng Med Bio 1994;13:487-496.
12. Nenonen J. Multimodal cardiac source imaging in the BioMag Laboratory. Bio Med Tech 1997;42(Suppl.1):29-32.
13. Saarinen M, Karp PJ, Katila TE, et al. The magnetocardiogram in cardiac disorders. Cardiovasc Res 1974;8:820-834.
14. Cohen D, Savard P, Rifkin RD, et al. Magnetic measurement of S-T and T-Q segment shifts in humans Part II: Exercise-induced S-T segment depression. Circ Res 1983; 53:274-279.
15. Cohen D, Kaufman LA. Magnetic determination of the relationship between the S-T-segment shift and the injury current produced by coronary artery occlusion. Circ Res 1975;36:414-424.
16. Cohen D, Norman JC, Molokhia F, et al. Magnetocardiography of direct currents: S-T segment and baseline shifts during experimental myocardial infarction. Science 1971; 172:1329-1333.
17. Lant J, Stroink G, ten Voorde B, et al. Complementary nature of electrocardiographic and magnetocardiographic data in patients with ischemic heart disease. J Electrocardiol 1990;23:315-322.
18. Cohen D, Hosaka H. Magnetic field produced by a current dipole. J Electrocardiol 1976;9:409-417.
19. Van Leeuwen P, Hailer B, Lange S, et al: Spatial and temporal changes during the QT-interval in the magnetic field of patients with coronary artery disease. Bio Med Tech 1999;44:139-142.
20. Lab MJ. Contraction-excitation feedback in myocardium: Physiological basis and clinical relevance. Circ Res 1982; 50:757-766.
21. Seese B, Moshage W, Achenbach S, et al. Magnetocardiographic (MCG) analysis of myocardial injury currents. Chapter in C Baumgartner, L Deecke, G Stroink (eds.): Biomagnetism: Fundamental Research and Clinical Applications. New York, Elsevier Science, 1995, pp. 628-632.
22. Hämäläinen MS, Nenonen J. Magnetic Source Imaging. Chapter in J.G. Webster (ed.): Encyclopedia of Electrical Engineering. New York, Wiley & Sons, in press.
23. Numminen J, Ahlfors S, Ilmoniemi R, et al. Transformation of multichannel magnetocardiographic signals to standard grid form. IEEE Trans Biomed Eng 1995;42:72-78.
24. Takala P, Hänninen H, Montonen J, et al. Magnetocardiographic and electrocardiographic exercise mapping in healthy subjects. Submitted.